Decay widths of large-spin mesons from the noncritical string/gauge duality

J. Sadeghi[1,2,*] and S. Heshmatian[1,†]

[1]*Sciences Faculty, Department of Physics, Mazandaran University, P. O. Box 47415-416, Babolsar, Iran*
[2]*Institute for Studies in Theoretical Physics and Mathematics (IPM), P. O. Box 19395-5531, Tehran, Iran*
(Received 13 June 2011; published 16 December 2011)

In this paper, we use the noncritical string/gauge duality to calculate the decay widths of large-spin mesons. Since it is believed that the string theory of QCD is not a ten-dimensional theory, we expect that the noncritical versions of ten-dimensional black hole backgrounds lead to better results than the critical ones. For this purpose we concentrate on the confining theories and consider two different six-dimensional black hole backgrounds. We choose the near-extremal AdS_6 model and the near-extremal KM model to compute the decay widths of large-spin mesons. Then, we present our results from these two noncritical backgrounds and compare them together with those from the critical models and experimental data.

DOI: 10.1103/PhysRevD.84.126010 PACS numbers: 11.25.Tq

I. INTRODUCTION

The gauge/gravity duality demonstrates the correspondence between a gravitational theory in anti-desitter space and a gauge theory at large N limit [1–6]. An example for this correspondence is the relation between type IIB string theory in ten-dimensional background and $\mathcal{N} = 4$ supersymmetric Yang-Mills theory on four-dimensional boundary of AdS_5. In recent years, using this correspondence as a powerful tool to study the QCD has been increased and lots of papers have been published in this context. For example, the dynamics of moving quark in a strongly coupled plasma [7–16] and the jet-quenching parameter [16–24] have been investigated. In addition, the motion of a quark-antiquark pair in the quark- gluon plasma has been studied in [25–31].

The calculations of decay widths of mesons are so important but they are hard to do by using the QCD methods because of the strong coupling problems. So, the holographic methods could help to overcome these difficulties. Recently, models including the various brane configurations have been introduced in critical dimensions to describe hadrons in the confining backgrounds. The model introduced in [32] is one example with $D4/D6$ brane configuration which leads to the heavy scaler and pseudoscalar mesons. Also, the model proposed by Sakai and Sugimoto [33] with $D4/D8/\overline{D8}$ in ten-dimensional background leads to a nice description of hadron physics. Many authors have used the holographic methods to study the hadron physics [34–36]. The decay process of mesons is a remarkable task which has been studied by using the SS model. The authors have calculated the meson masses and the decay rates by consideration of low-spin meson as small fluctuations of flavor branes. Of course, these models can be used only for low-spin mesons and can not describe the large-spin mesons anymore.

Large-spin mesons are interesting because of their phenomenological features, therefore some authors have chosen the dual string theory description to study their decay processes in critical dimentions [37]. In this paper, an interesting setup has been proposed to compute the decay widths of mesons. They have used a semiclassical U-shaped spinning string configuration. This string can decay into some outgoing mesons by touching one or more of the flavor branes, splitting and then getting reconnected to the brane due to the quantum fluctuations. The idea in this paper is to focus on the near-wall geometry and build the string-wave function near in this geometry by semiclassical quantization. The authors compared their results with the Casher-Neuberger-Nussinov model where quark-antiquark pairs are connected by a chromoelectric flux tube [38].

There is also an old model called the ‘‘Lund model’’ describing the mesons decay [39]. There are improvements for this model in the literature where two massive quarks are connected together by a massless relativistic string [40]. The resulting formula leads to a better description for the decay widths. It shows that for a decay width linear in length, the ratio of Γ/M is not a constant anymore. Also, the decay process of the open strings [41] and closed strings [42] is studied before by using different methods.

The decay widths of both low-spin and large-spin mesons has been studied in critical dimensions [33,37]. Also, some calculations for the low-spin mesons have been done before by using the noncritical string/gauge duality [43]. But the decay widths of high spin mesons has not been studied in the context of the noncritical dual mesons yet. In holographic QCD, there is an idea that the string theory in dimensions less than ten is a good candidate to study the QCD. So, this motivates us to study the decay widths of large-spin mesons by using the noncritical version of ten-dimensional black hole backgrounds [43–49]. For this purpose, we consider two different six-dimensional backgrounds. The first one is the near-extremal flavored AdS_6, which is dual to a four-dimensional low energy effective

*pouriya@ipm.ir
†s.heshmatian@umz.ac.ir

 © 2011 American Physical Society

gauge theory. Mesons in the ir theory are constructed by the quarks with a mass of the order of temperature. This model is based on the near-extremal D_4 branes background and the D_6 flavor branes added to this background. The second one is the same as the Klebanov-Maldacena model called KM model [47] with flavored $AdS_5 \times S^1$ background. In the near-extremal background, there is a system of D_3 and uncharged D_5 branes in six-dimensional string theory and one of the gauge theory flat directions is compact on a thermal circle in order to break supersymmetry [43]. The near-extremal solution is dual to the four-dimensional theory at finite temperature without supersymmetry and conformal invariance. In this paper, we use the semiclassical model introduced in Ref. [37] and do the same calculations in the two noncritical dual pictures. For this purpose, we choose the flat space-time approximation for simplicity. According to Ref. [37], we construct the wave function for the string configuration and use it to compute the decay width. This paper is organized as follows: In Sec. II we use the noncritical AdS_6 background to write an expression for the meson decay width.

In Sec. III we use another noncritical background, the near-extremal KM model with $AdS_5 \times S^1$ black hole, and obtain another equation for the meson decay width for six-dimensional string theory. In the last section, we present our numerical results and compare them with the previous models and the experimental data of Ref. [50]. Also, we use the modified relation between the length of horizontal part of the string and its mass derived in [40] and obtain the decay widths for two noncritical backgrounds of Secs. II and III and compare them with the data.

II. DECAY WIDTHS IN THE NEAR-EXTREMAL AdS_6 MODEL

In this paper, we use two different noncritical backgrounds to calculate the mesons decay widths: the near-extremal AdS_6 model in this section and the near-extremal Klebanov-Maldacena model with $AdS_5 \times S^1$ background in the next section. Also, we use the method proposed in Ref. [37] for the critical dimensions to calculate the decay widths. First, we briefly review the model of Ref. [37] and then use it to do our calculations. In this paper, a semiclassical U-shaped spinning string configuration with two massive endpoints on the flavor brane is considered. The string is pulled toward the infrared wall and also extends along it. This configuration is equivalent to a high spin meson with massive quarks.

The string can decay into some outgoing mesons by touching one or more of the flavor branes, splitting and then getting reconnected to the branes due to the quantum fluctuations. The idea in this paper is to focus on the near-wall geometry and build the string-wave function near in this geometry by semiclassical quantization. The total wave function for a classical U-shaped string is [37]

$$\Psi[\{\mathcal{N}_n\}] = \prod_n \Psi_n[\mathcal{N}_n(X^M)]. \tag{1}$$

Where $\mathcal{N}_n(X^M)$ are normal coordinates, X^M are the target space coordinates and $\Psi_n[\mathcal{N}_n(X^M)]$ are the wave function of normal modes $\mathcal{N}_n$. Because of the quantum fluctuations, the string may touch the flavor brane in one or more points with the probability given by [37]

$$\mathcal{P}_{\text{fluct}} = \int'_{\{\mathcal{N}_n\}} |\Psi[\{\mathcal{N}_n\}]|^2, \tag{2}$$

and only the configurations with the following condition are being integrated

$$\max(U(\sigma)) \geq U_B. \tag{3}$$

The splitting probability for the string to is given by [37]

$$\mathcal{P}_{\text{split}} b := \frac{1}{T_{\text{eff}}} \frac{\Gamma_{\text{open}}}{L}. \tag{4}$$

Using this relation, the total decay width takes this form

$$\Gamma = T_{\text{eff}} \mathcal{P}_{\text{split}} \times \int'_{\{\mathcal{N}_n\}} |\Psi[\{\mathcal{N}_n\}]|^2 K[\{\mathcal{N}_n\}], \tag{5}$$

where $K[\{\mathcal{N}_n\}]$ is a factor with the dimension of L which measures the size of string sesments intersect the flavor brane. Finally, the authors in Ref. [37] obtained the approximated decay width as following

$$\Gamma_{\text{approx}} = (T_{\text{eff}} \mathcal{P}_{\text{split}} \times L \times \kappa_{\max}) \times \mathcal{P}_{\text{fluct}}, \tag{6}$$

where $\kappa_{\max}$ is dimensionless. The fluctuation probability is the main thing that should be computed for the decay width. $\mathcal{P}_{\text{fluct}}$.

Now, we are going to use the procedure proposed in Ref. [37] to evaluate the decay widths. First, we use the model introduced above to calculate the meson decay width in the near-extremal AdS_6 black hole background [43]. This background is constructed by near-extremal color $D4$-branes and additional $D4/\overline{D4}$ flavor branes. In order to have a nonsupersymmetric gauge theory with massless fundamentals, $D4$ flavor branes are added to the background which are extended along the Minkowski directions and stretched along the radial direction. The background metric has the form

$$ds_6^2 = \left(\frac{U}{R_{\text{AdS}}}\right)^2 dx_{1,3}^2 + \left(\frac{R_{\text{AdS}}}{U}\right)^2 \frac{dU^2}{f(U)} + \left(\frac{U}{R_{\text{AdS}}}\right)^2 f(U) d\theta^2, \tag{7}$$

$$F_{(6)} = Q_c \left(\frac{U}{R_{\text{AdS}}}\right)^4 dx_0 \wedge dx_1 \wedge dx_2 \wedge dx_3 \wedge dU \wedge d\theta \tag{8}$$

$$e^{\phi} = \frac{2\sqrt{2}}{\sqrt{3} Q_c}, \qquad R_{\text{AdS}}^2 = \frac{15}{2}, \tag{9}$$

where ϕ is a constant dilaton, $F_{(6)}$ is the RR six-form field strength and

$$f(U) = 1 - \left(\frac{U_\Lambda}{U}\right)^5. \tag{10}$$

The coordinate θ should be periodic in order to avoid a conical singularity on the horizon

$$\theta \sim \theta + \delta\theta, \qquad \delta\theta = \frac{4\pi R_{\rm AdS}^2}{5U_\Lambda}, \tag{11}$$

where $L_\Lambda \equiv \delta\theta$ is the size of the thermal circle and should be small in order to have a dual four-dimensional low energy effective gauge theory [32]. The mass scale for this noncritical metric is

$$M_\Lambda = \frac{2\pi}{\delta\theta} = \frac{5}{2}\frac{U_\Lambda}{R_{\rm AdS}^2}. \tag{12}$$

At leading order, the fluctuations of horizontal part of the string on the wall experiences a flat geometry. First, we use the following coordinate to see when the flat approximation is valid [37]

$$\eta^2 = \frac{U - U_\Lambda}{U_\Lambda}. \tag{13}$$

Then, we expand the metric of Eq. (7) around $\eta = 0$ to quadratic order and find the following expression for the AdS_6 metric

$$ds^2 \sim \left(\frac{U_\Lambda}{R_{\rm AdS}}\right)^2 (1 + 2\eta^2)(\eta_{\mu\nu} dX^\mu dX^\nu) + \frac{4}{5} R_{\rm AdS}^2 d\eta^2 + 5\left(\frac{U_\Lambda}{R_{\rm AdS}}\right)^2 \eta^2 d\theta^2. \tag{14}$$

Then, we consider the following solutions of a rotating string at the ir wall

$$\begin{aligned} T &= L\tau, & X^1 &= L \sin\tau \sin\sigma, \\ X^2 &= L\cos\tau \sin\sigma, & U &= U_\Lambda, \end{aligned} \tag{15}$$

where L is the length of the horizontal part of the string. To quantize the linearized metric (14) by using the Polyakov formulation. The Polyakov string action in a curved background is given by

$$S = \frac{1}{2\pi\alpha'} \int d\tau \int_0^{2\pi\sqrt{\alpha'}} d\sigma G_{MN} [\dot{X}^M \dot{X}^N - X^{M\prime} X^{N\prime}]. \tag{16}$$

As explained in Ref. [37], the fluctuations along the wall directions are irrelevant to construct the wave function. So, we only consider the fluctuations in the η and X^μ directions (transverse to the wall). By expanding the above action around the solutions of (15) and keeping the quadratic terms in η, we find the following action

$$\begin{aligned} S = \frac{1}{2\pi\alpha'}\left(\frac{U_\Lambda}{R_{\rm AdS}}\right)^2 \int d\tau d\sigma \frac{4}{5}\frac{R_{\rm AdS}^4}{U_\Lambda^2}[(\dot{\eta}^2 - \eta'^2) \\ - b\cos^2(\sigma)(1 + 2\eta^2)] + [(1 + 2\eta^2) \\ \times (\delta\dot{X}^\mu \delta\dot{X}^\nu \eta_{\mu\nu} - \delta X^{\mu'} \delta X^{\nu'} \eta_{\mu\nu})], \end{aligned} \tag{17}$$

where b is a dimensionless parameter as following

$$b \equiv \frac{5}{2}\frac{\pi^2 L^2 U_\Lambda^2}{R_{\rm AdS}^4}, \tag{18}$$

which determines the effect of curvature. If $b \ll 1$, the string fluctuations are small enough, so we can use the flat space approximation with the following coordinate

$$\eta = \sqrt{\frac{5}{4}}\frac{U_\Lambda}{R_{\rm AdS}^2} z. \tag{19}$$

to write the metric (14) in the conformally flat form.

$$ds^2 \sim \left(\frac{U_\Lambda}{R_{\rm AdS}}\right)^2 (\eta_{\mu\nu} dX^\mu dX^\nu + dz^2) + 5\left(\frac{U_\Lambda}{R_{\rm AdS}}\right)^2 \eta^2 d\theta^2. \tag{20}$$

Again, by expanding the Polyakov action for the fluctuations in the directions transverse to the wall and use $T = L\tau$, we find

$$S_{\rm fluct} = \frac{L}{2\pi\alpha'_{\rm eff(1)}} \int dT d\sigma \left[-(\partial_T z)^2 + \frac{1}{L^2}(\partial_\sigma z)^2\right], \tag{21}$$

where we have neglected the fluctuations in the directions along the wall. In the above formula, the string effective coupling for the near-extremal AdS_6 background is as following

$$\alpha'_{\rm eff(1)} = \alpha' \left(\frac{R_{\rm AdS}}{U_\Lambda}\right)^2, \tag{22}$$

which is obtained by using the following equation for the noncritical string stretching close to the horizon of the AdS_6 black hole [43]

$$T_{\rm eff(1)} = \frac{1}{2\pi\alpha'}\sqrt{g_{00} g_{xx}}|_{\rm wall} = \frac{1}{2\pi\alpha'}\left(\frac{U_\Lambda}{R_{\rm AdS}}\right)^2. \tag{23}$$

Then, by imposing the Dirichlet boundary conditions for the fluctuations $z(\sigma, \tau)$, one can write the following equation

$$z(\sigma, \tau) = \sum_{n>0} z_n \cos(n\sigma). \tag{24}$$

We put this in the action (21) and integrate over σ coordinate to obtain

$$S_{\rm fluct} = \frac{L}{2\alpha'_{\rm eff(1)}} \int dT \Big[\sum_{n>0} \Big(-(\partial_T z_n)^2 + \frac{n^2}{L^2} z_n^2 \Big) \Big] \quad (25)$$

for the fluctuation in the z direction. From this equation, we can easily find that the system is similar to infinite number of linear harmonic oscillators. The frequencies are n/L and the masses are $L/\alpha'_{\rm eff(1)}$. We can see that this result is in the form of the critical setup obtained in Ref. [37]. But the important difference is in the expression of $\alpha'_{\rm eff(1)}$ (Eq. (22)), which is different in critical and noncritical cases. Also, the values of U_Λ and $R^2_{\rm AdS}$ differ from the corresponding critical values. The wave function in the factorized form is [37]

$$\Psi(\{z_n\}, \{x_n\}) = \Psi_{\rm long}(\{x_n\}) \times \Psi_{\rm sphere}(\{y_n\}) \times \Psi_\theta(\{\theta_n\}) \times \Psi_{\rm trans}(\{z_n\}) \quad (26)$$

where $\Psi_{\rm long} = \Psi_{\rm sphere} = \Psi_\theta = 1$ because only the fluctuations transverse to the wall contribute to the fluctuation probability, and those belong to other directions are being integrated. So the wave function for the transverse directions is written as [37]

$$\Psi[\{z_n\}] = \prod_{n=1}^{\infty} \Psi_0(z_n). \quad (27)$$

From Eq. (25) we can write the following equation for the wave functions of the string compared to the harmonic oscillators

$$\Psi_0(z_n) = \Big(\frac{n}{\pi \alpha'_{\rm eff(1)}} \Big)^{1/4} \exp\Big(-\frac{n}{2\alpha'_{\rm eff(1)}} z_n^2 \Big). \quad (28)$$

This equation is also similar to the critical case [37], but the difference is in the $\alpha'_{\rm eff(1)}$ equation. All oscillators are in their ground state and there is no relevant excited mode. Also, there is the following condition [37]

$$\sum_{n>0} |z_n| \le z_B, \quad (29)$$

which means that if one add all the modes constructively, the total amplitude is still smaller than z_B. This condition leads to the following expression for the upper bound on the fluctuation probability [37]

$$\mathcal{P}^{\rm max}_{\rm fluct} = 1 - \int_{\sum_{n>0}} \cdots \int_{|z_n| \le z_B} \prod_{n=1}^{\infty} dz_n |\Psi(\{z_n\})|^2. \quad (30)$$

There is also another condition for the string not to touch the brane which leads to a lower bound for the string fluctuation probability as following [37]

$$\mathcal{P}^{\rm min}_{\rm fluct} = 1 - \lim_{N\to\infty} \int_0^{z_B} dz_1 \times \int_0^{z_B} dz_2 \cdots \int_0^{z_B} dz_N |\Psi(\{z_n\})|^2. \quad (31)$$

The authors in Ref. [37] have evaluated this integral numerically and fitted their result to a Gaussian with the following expression:

$$\mathcal{P}^{\rm min}_{\rm fluct} \approx \exp\Big(-1.3 \frac{z_B^2}{\alpha'_{\rm eff}} \Big). \quad (32)$$

They have obtained this result by using the $\mathcal{P}^{\rm min}_{\rm fluct}$ plot in terms of $z_B/\sqrt{\alpha'_{\rm eff}}$. If we do the same process, the following equation for $\mathcal{P}^{\rm min}_{\rm fluct}$ is obtained

$$\mathcal{P}^{\rm min}_{\rm fluct} \approx \exp\Big(-1.3 \frac{z_B^2}{\alpha'_{\rm eff(1)}} \Big). \quad (33)$$

This equation is the same as Ref. [37], except that the $\alpha'_{\rm eff}$ is replaced by $\alpha'_{\rm eff(1)}$. Then we put Eq. (33) into the Eq. (6) and find the decay width of large-spin mesons in the flat space approximation as following

$$\Gamma_{\rm flat} = ({\rm const} \times T_{\rm eff} \mathcal{P}_{\rm split} \times L) \times \exp\Big(-1.3 \frac{z_B^2}{\alpha'_{\rm eff(1)}} \Big). \quad (34)$$

This is the decay width we obtain by using the near-extremal AdS_6 black hole background. The difference between our result and the result of critical dimensions (Ref. [37]) is the precise form of the exponent. Since the string effective coupling is different in these two backgrounds, this leads to different results for the decay width. Also, this difference exists in the case of the Lund model [39]. We present our numerical results in the last section. Equation (34) shows that the ratio Γ/L is constant on the same Regge trajectory just like the results of the Ref. [37] and the Lund model. But the experimental data do not support this result exactly. As mentioned in Ref. [37], this deviation could be justify by the fact that the Regge trajectories in the nature are not straight lines and one should consider the effect of two massive endpoints as following: [40]

$$\frac{L}{M} = \frac{2}{\pi T_{\rm eff}} - \frac{m_1 + m_2}{2T_{\rm eff} M} + \mathcal{O}\Big(\frac{m_i^2}{M^2} \Big). \quad (35)$$

In Ref. [37], this relation has been applied to the decay rates. The authors showed that in the case of Γ linear in L, the Γ/M ratio in not a constant. They concluded that as M increase, this ratio increases and reaches to a universal value for large M. So, Eq. (35) leads to a better result for the decay width which is compatible with the experimental data. We also use this equation together with Eq. (22) to find the decay widths for a and f mesons. We discuss our results in the last section.

III. DECAY WIDTHS IN THE NEAR-EXTREMAL *KM* MODEL

In this section, we use another noncritical background to compute the decay width of large-spin mesons. We choose the near-extremal version of Klebanov-Maldacena model, $AdS_5 \times S^1$. The system is composed of $D3$ color branes and uncharged $D5$ flavor branes in six-dimensional noncritical string theory. Here, we consider one of gauge theory flat dimensions to be compact on a thermal circle. This background is dual to a four-dimensional field theory at finite temperature with fundamental flavors. The $AdS_5 \times S^1$ metric is given by [43]

$$ds^2 = \left(\frac{U}{R'_{\mathrm{AdS}}}\right)^2\left(dx_{1,2}^2 + \left(1 - \left(\frac{U_\Lambda}{U}\right)^4\right)d\theta^2\right) + \left(\frac{R'_{\mathrm{AdS}}}{U}\right)^2\frac{dU^2}{1 - (\frac{U_\Lambda}{U})^4} + R_{S^1}^2 d\varphi^2, \tag{36}$$

with $R'_{\mathrm{AdS}} = \sqrt{6}$, $R_{S^1}^2 = \frac{4Q_c^2}{3Q_f^2}$, $U_\Lambda^4 = 2b_1 R'^4_{\mathrm{AdS}}$ and $e^{\phi_0} = \frac{4}{3Q_f}$. The RR 5-form field strength is

$$F_5 = Q_c\left(\frac{U}{R'_{\mathrm{AdS}}}\right)^3 dx^0 \wedge dx^1 \wedge dx^2 \wedge d\theta \wedge dU, \tag{37}$$

and the period of the compact direction θ is as following:

$$\theta \sim \theta + \frac{\pi R'^2_{\mathrm{AdS}}}{U_\Lambda}. \tag{38}$$

Again, we use the coordinate of Eq. (15) to expand the metric (36) around $\eta = 0$ just like what we did in the previous section. Then we find

$$ds^2 \sim \left(\frac{U_\Lambda}{R'_{\mathrm{AdS}}}\right)^2(1 + 2\eta^2)(\eta_{\mu\nu}dX^\mu dX^\nu) + R'^2_{\mathrm{AdS}}d\eta^2 + 4\left(\frac{U_\Lambda}{R'_{\mathrm{AdS}}}\right)^2\eta^2 d\theta^2 + R_{S^1}^2 d\varphi^2. \tag{39}$$

Then we consider fluctuations in the directions transverse to the wall and expand the Polyakov action (16) around the solutions (15). By keeping quadratic terms in η, we obtain the following action

$$S = \frac{1}{2\pi\alpha'}\left(\frac{U_\Lambda}{R'_{\mathrm{AdS}}}\right)^2\int d\tau d\sigma \frac{R'^4_{\mathrm{AdS}}}{U_\Lambda^2}[(\dot\eta^2 - \eta'^2) - b'\cos^2(\sigma)(1 + 2\eta^2)] + [(1 + 2\eta^2) \times (\delta\dot X^\mu \delta\dot X^\nu \eta_{\mu\nu} - \delta X^{\mu'}\delta X^{\nu'}\eta_{\mu\nu})], \tag{40}$$

where the dimensionless parameter b' is

$$b' \equiv \frac{2L^2U_\Lambda^2}{R'^4_{\mathrm{AdS}}}. \tag{41}$$

In the case of $b' \ll 1$, we have the flat space approximation because the fluctuations of the string are small. Then we can use the coordinate

$$z = \frac{R'^2_{\mathrm{AdS}}}{U_\Lambda}\eta, \tag{42}$$

to write the metric (40) in the following conformally flat form

$$ds^2 \sim \left(\frac{U_\Lambda}{R'_{\mathrm{AdS}}}\right)^2(\eta_{\mu\nu}dX^\mu dX^\nu + dz^2) + \left(\frac{U_\Lambda}{R'_{\mathrm{AdS}}}\right)^2\eta^2 d\theta^2 + R_{S^1}^2 d\varphi^2. \tag{43}$$

Again, when we expand the Polyakov action for the fluctuations in the transverse directions and use $T = L\tau$, we can find

$$S_{\mathrm{fluct}} = \frac{L}{2\pi\alpha'_{\mathrm{eff}(2)}}\int dTd\sigma\left[-(\partial_T z)^2 + \frac{1}{L^2}(\partial_\sigma z)^2\right], \tag{44}$$

where

$$\alpha'_{\mathrm{eff}(2)} = \alpha'\left(\frac{R'_{\mathrm{AdS}}}{U_\Lambda}\right)^2 \tag{45}$$

is the effective string coupling for the near-extremal *KM* model. Because of the AdS radii differences in these two noncritical backgrounds, this equation is not the same as Eq. (22). Then we put Eq. (24) for the fluctuations $z(\sigma, \tau)$ into the action (44) and integrate over σ coordinate to find

$$S_{\mathrm{fluct}} = \frac{L}{2\alpha'_{\mathrm{eff}(2)}}\int dT\left[\sum_{n>0}\left(-(\partial_T z_n)^2 + \frac{n^2}{L^2}z_n^2\right)\right]. \tag{46}$$

This action is also similar to the action for an infinite number of linear harmonic oscillators with frequencies n/L and masses $L/\alpha'_{\mathrm{eff}(2)}$. Then by using the process of previous section, we find the string fluctuation probability as following

$$\mathcal{P}^{\min}_{\mathrm{fluct}} \approx \exp\left(-1.3\frac{z_B^2}{\alpha'_{\mathrm{eff}(2)}}\right). \tag{47}$$

By inserting Eq. (47) into Eq. (6), we obtain the following equation for the decay width of large-spin mesons in the near-extremal *KM* model:

$$\Gamma_{\mathrm{flat}} = (\mathrm{const} \times T_{\mathrm{eff}}\mathcal{P}_{\mathrm{split}} \times L) \times \exp\left(-1.3\frac{z_B^2}{\alpha'_{\mathrm{eff}(2)}}\right), \tag{48}$$

where z_B is the position of the flavor brane. This equation is for the flat space approximation and is similar to the

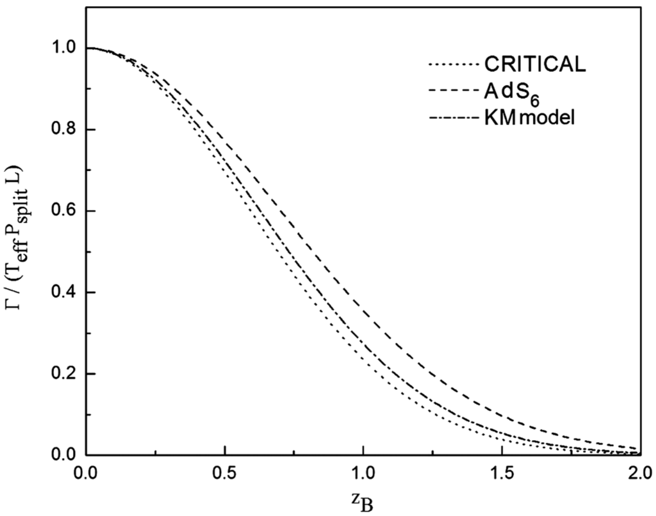

FIG. 1. The decay widths of mesons vs the position of flavor brane. The dashed line belongs to the AdS_6 model, the dashed-dotted line belongs to the near-extremal KM model, and the dotted line is for the critical case. The decay width in the noncritical models are more than the critical one.

near-extremal AdS_6 results and also Ref. [37]. These results are different in the precise form of the exponent which depend on effective string couplings. This is the decay width obtained by using the near-extremal KM model with the $AdS_5 \times S^1$ black hole background. We present our numerical results in the last section.

IV. RESULTS AND DISCUSSION

In this section, we present the numerical results for the decay widths and compare them with the models in [37] and the experimental data of Ref. [50].

As mentioned before, the difference between Eqs. (34) and (48) and the critical model [37] is the different effective string couplings. We use these equations and obtain the decay widths numerically. For this purpose, we put the values $R_{\mathrm{AdS}} = \sqrt{\frac{15}{2}}$, $R'_{\mathrm{AdS}} = \sqrt{6}$, and $T_{\mathrm{eff(cr)}} = 0.177$ into the Eqs. (34) and (48) and use Eqs. (22) and (45) to plot the decay width (Fig. 1). From this diagram, we can see that the decay widths of mesons in the noncritical backgrounds of Secs. II and III are more than in the critical model. So we find larger values for the decay widths compared to the critical model.

Then we plot Γ/M in terms of M for two large-spin mesons, a and f by using a sigmoidal fitting for the experimental data of Ref. [50] (see Fig. 2). From this diagram, we can see that the decay widths in the nature are not constant on the same Regge trajectory. The decay widths behave like Eq. (35) in which the effect of two massive endpoints of the string is considered.

Also, we can use Eq. (35) for the two noncritical models of sections II and III and the critical model [37] to plot Γ/M in terms of M (Fig. 3). In this figure, we can see that for the a trajectory, there is a good agreement between the AdS_6 diagram and the experimental data for all spin values (the left diagram). For the f trajectory we can see that our results deviate from the experimental results in low spins and the fitting of experimental data has a better agreement with the critical model of Ref. [37] but for high spins in the f trajectory, the $AdS_5 \times S^1$ diagram is more compatible with the experimental data (the right diagram).

In this paper, we used the noncritical string/gauge duality and obtained the decay widths for large-spin mesons. We chose two different six-dimensional black hole backgrounds; the near-extremal AdS_6 background and

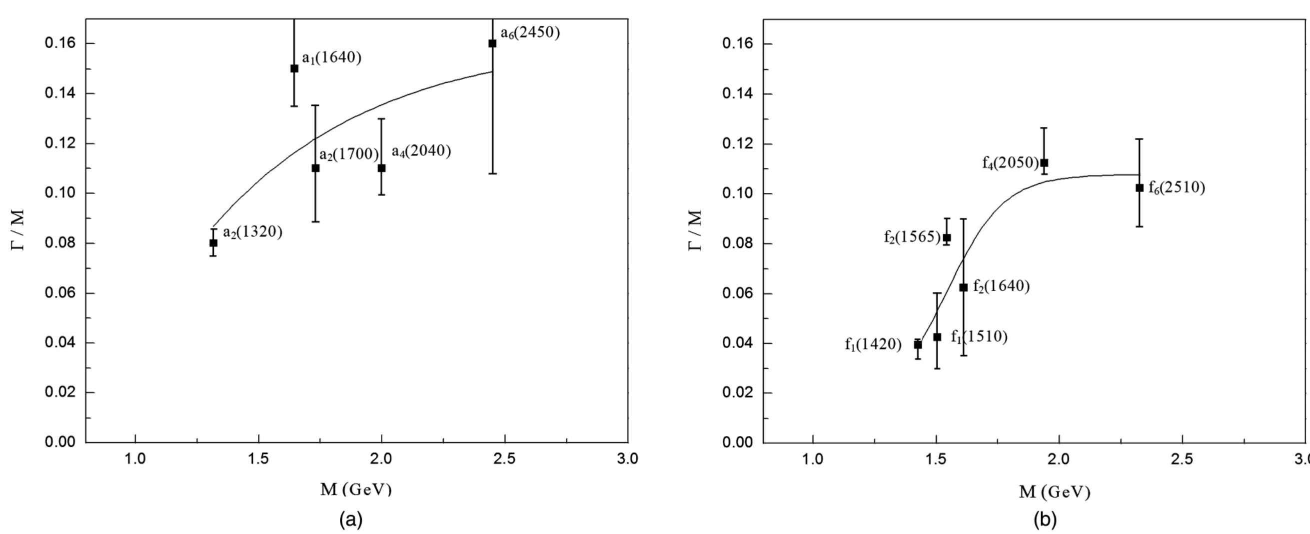

FIG. 2. a) The decay width divided by mass versus the mass of the mesons states on the a trajectory. b) The decay width divided by mass versus the mass of the mesons states on the f trajectory. The solid lines correspond to a sigmoidal fitting for the data [50].

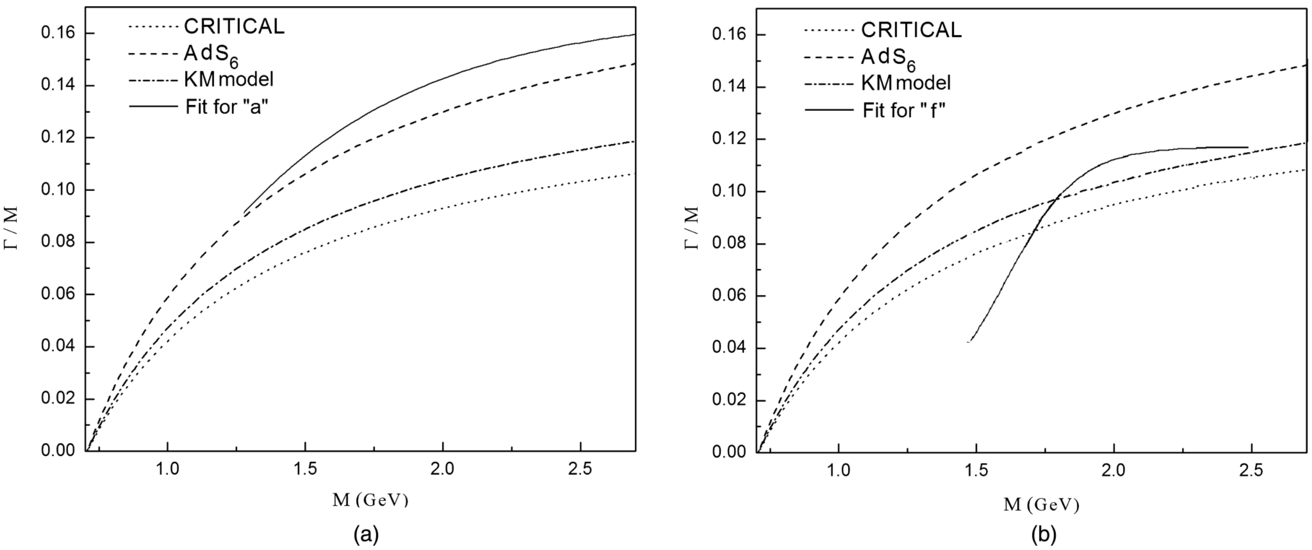

FIG. 3. a) Comparison of the Γ/M vs M for two noncritical models, critical model [37], and the fitting for a meson. The dashed line belongs to the AdS_6 model, the dashed-dotted line belongs to the $AdS_5 \times S^1$ KM model, and the dotted line is for the critical case. The solid line is the fit for a meson. b) Comparison of the Γ/M vs M for two noncritical models, critical model [37], and the fitting for f meson.

the near-extremal KM model. By using the method of Ref. [37], we obtained expressions for the decay widths and plotted it in terms of the position of the flavor brane (Fig. 1). From this diagram it is easy to see that the noncritical models lead to larger values for the decay width. Then we used another equation from Ref. [40] and plotted the decay width in terms of the masses of meson states. We compared these results with the fitting of experimental data of Ref. [50] for mesons a and f (Fig. 3). From these diagrams, one can find that for a meson, the AdS_6 background leads to a better result. Also, for f meson, the near-extremal KM model has better agreement with data only for large spins. For lower spins, the critical model of Ref. [37] is closer to the experimental data.

[1] J.M. Maldacena, Adv. Theor. Math. Phys. **2**, 231 (1998).
[2] E. Witten, Adv. Theor. Math. Phys. **2**, 253 (1998).
[3] J.H. Schwarz, *Introduction to M Theory and AdS/CFT Duality*, Lecture Notes in Physics (Springer, Berlin, 1999), Vol. 525, pp. 1–21.
[4] M.R. Douglas and S. Randjbar-Daemi, arXiv:hep-th/9902022.
[5] J.L. Petersen, Int. J. Mod. Phys. A **14**, 3597 (1999).
[6] R. Klebanov Igor, arXiv:hep-th/0009139.
[7] C.P. Herzog, A. Karch, P. Kovtun, C. Kozcaz, and L.G. Yaffe, J. High Energy Phys. 07 (2006) 013.
[8] C.P. Herzog, J. High Energy Phys. 09 (2006) 032.
[9] S.S. Gubser, Phys. Rev. D **74**, 126005 (2006).
[10] J.F. Vazquez-Poritz, arXiv:0803.2890.
[11] E. Caceres and A. Guijosa, J. High Energy Phys. 11 (2006) 077.
[12] T. Matsuo, D. Tomino, and W.Y. Wen, J. High Energy Phys. 10 (2006) 055.
[13] J. Sadeghi, M.R. Setare, and B. Pourhassan, J. Phys. G **36**, 115005 (2009) (19pp).
[14] J. Sadeghi, M.R. Setare, B. Pourhassan, and S. Hashmatian, Eur. Phys. J. C **61**, 527 (2009).
[15] J. Sadeghi and B. Pourhassan, J. High Energy Phys. 12 (2008) 026.
[16] E. Nakano, S. Teraguchi, and W.Y. Wen, Phys. Rev. D **75**, 085016 (2007).
[17] H. Liu, K. Rajagopal, and U.A. Wiedemann, Phys. Rev. Lett. **97**, 182301 (2006).
[18] J.F. Vazquez-Poritz, arXiv:hep-th/0605296.
[19] E. Caceres and A. Guijosa, J. High Energy Phys. 12 (2006) 068.
[20] F.L. Lin and T. Matsuo, Phys. Lett. B **641**, 45 (2006).
[21] S.D. Avramis and K. Sfetsos, J. High Energy Phys. 01 (2007) 065.
[22] N. Armesto, J.D. Edelstein, and J. Mas,J. High Energy Phys. 09 (2006) 039.
[23] J.D. Edelstein and C.A. Salgado, AIP Conf. Proc. **1031**, 207 (2008).
[24] K.B. Fadafan, Eur. Phys. J. C **68**, 505 (2010).
[25] K. Peeters, J. Sonnenschein, and M. Zamaklar, Phys. Rev. D **74**, 106008 (2006).
[26] H. Liu, K. Rajagopal, and U.A. Wiedemann, Phys. Rev. Lett. **98**, 182301 (2007).
[27] M. Chernicoff, J.A. Garcia, and A. Guijosa, J. High Energy Phys. 09 (2006) 068.

[28] J. Erdmenger, N. Evans, I. Kirsch, and E. J. Threlfall, Eur. Phys. J. A **35**, 81 (2008).

[29] J. Sadeghi and S. Heshmatian, Int. J. Theor. Phys. **49**, 1811 (2010).

[30] M. Ali-Akbari and K. B. Fadafan, Nucl. Phys. **B835**, 221 (2010).

[31] M. Chernicoff, J. A. Garcia, and A. Guijosa, J. High Energy Phys. 09 (2006) 068.

[32] E. Witten, Adv. Theor. Math. Phys. **2**, 505 (1998).

[33] T. Sakai and S. Sugimoto, Prog. Theor. Phys. **113**, 843 (2005); Prog. Theor. Phys. **114**, 1083 (2005); K Hashimoto, T. Sakai, and S. Sugimoto, Prog. Theor. Phys. **120**, 1093 (2008); H. Hata, T. Sakai, S. Sugimoto, and S. Yamato, Prog. Theor. Phys. **117**, 1157 (2007).

[34] K. Y. Kim, S. J. Sin, and I. Zahed, J. High Energy Phys.01 (2008) 002; O. Bergmann, G. Lifschytz, and M. Lippert, J. High Energy Phys. 11 (2007)056.

[35] M. Kruczenski, L. A P. Zayas, J. Sonnenschein, and D. Vaman, J. High Energy Phys. 06 (2005) 046.

[36] M. Rozali *et al.*, J. High Energy Phys. 01 (2008) 053; S. J. Sin, S. Yang, and Y. Zhou, J. High Energy Phys. 11 (2009) 001; G. Curtis *et al.*, Nucl. Phys. **B547**, 127 (1999).

[37] K. Peeters, J. Sonnenschein, and M. Zamaklar, J. High Energy Phys. 02 (2006) 009.

[38] A. Casher, H. Neuberger, and S. Nussinov, Phys. Rev. D **20**, 179 (1979).

[39] T. Sjöstrand, Comput. Phys. Commun. **27**, 243 (1982); B. Andersson, *The Lund Model* (Cambridge University Press, Cambridge, England 1998); B. Andersson *et al.*, Phys. Rep. **97**, 31 (1983).

[40] M. Ida, Prog. Theor. Phys. **59**, 1661 (1978).

[41] L. A. Cotrone, L. Martucci, and W. Troost, Phys. Rev. Lett. **96**, 141601 (2006); J. Dai and J. Polchinski, Phys. Lett. B **220**, 387 (1989); K. S. Gupta and C. Rosenzweig, Phys. Rev. D **50**, 3368 (1994); K. Peeters, J. Plefka, and M. Zamakler, J. High Energy Phys. 11 (2004) 054.

[42] R. B. Wilkinson, N. Turok, and D. Mitchell, Nucl. Phys. **B332**, 131 (1990).

[43] R. Casero, A. Paredes, and J. Sonnenschein, J. High Energy Phys. 01 (2006) 127.

[44] S. Kuperstein and J. Sonnenschein, J. High Energy Phys. 07 (2004) 049.

[45] F. Bigazzi *et al.*, J. High Energy Phys. 10 (2005) 012.

[46] A. Giveon, D. Kutasov, and O. Pelc, J. High Energy Phys. 10 (1999) 035.

[47] I. R. Klebanov and J. M. Maldacena, Int. J. Mod. Phys. A **19**, 5003 (2004).

[48] S. Kuperstein and J. Sonnenschein, J. High Energy Phys. 11 (2004) 026.

[49] G. Ferretti, J. Kalkkinen, and D. Martelli, Nucl. Phys. **B555**, 135 (1999); A. Armoni, E. Fuchs, and J. Sonnenschein, J. High Energy Phys. 06 (1999) 027; K. Ghoroku, J. Phys. G **26**, 233 (2000); E. Alvarez, C. Gomez, and L. Hernandez, Nucl. Phys. **B600**, 185 (2001); S. Murthy, J. High Energy Phys. 11 (2003) 056; A. Fotopoulos, V. Niarchos, and N. Prezas, J. High Energy Phys. 10 (2005) 081; S. K. Ashok, S. Murthy, and J. Troost, Nucl. Phys. **B749**, 172 (2006); P. A. Grassi and Y. Oz, arXiv:hep-th/0507168.

[50] K. Nakamura *et al.* (Particle Data Group) J. Phys. G **37**, 075021 (2010).